

We are IntechOpen, the world's leading publisher of Open Access books Built by scientists, for scientists

5,800

Open access books available

142,000

International authors and editors

180M

Downloads

Our authors are among the

154

Countries delivered to

TOP 1%

most cited scientists

12.2%

Contributors from top 500 universities



WEB OF SCIENCE™

Selection of our books indexed in the Book Citation Index
in Web of Science™ Core Collection (BKCI)

Interested in publishing with us?
Contact book.department@intechopen.com

Numbers displayed above are based on latest data collected.
For more information visit www.intechopen.com



Light Weight Complex Metal Hydrides for Reversible Hydrogen Storage

*Sesha Srinivasan, Luis Rivera, Diego Escobar
and Elias Stefanakos*

Abstract

We have investigated the complex metal hydrides involving light weight elements or compounds for the reversible hydrogen storage. The complex hydrides are prepared via an inexpensive solid state mechanochemical process under reactive atmosphere at ambient temperatures. The complex metal hydride, LiBH_4 with different mole concentrations of ZnCl_2 were characterized for the new phase formation and hydrogen decomposition characteristics of $\text{Zn}(\text{BH}_4)_2$. Furthermore, the complex metal hydride is destabilized using the addition of nano MgH_2 for the reversible hydrogen storage characteristics. The structural, microstructural, surface, and other physicochemical behaviors of these lightweight complex metal hydrides have been studied via various metrological tools such as x-ray diffraction, Fourier transform infrared spectroscopy, thermal programmed desorption, and PCT hydrogen absorption methods.

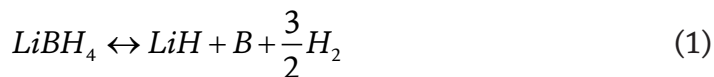
Keywords: hydrogen storage, mechanochemistry, complex metal hydrides, hydrogen sorption, thermal decomposition

1. Introduction

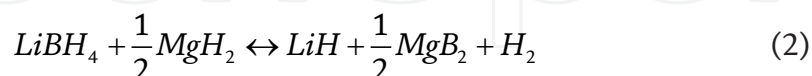
Complex metal hydrides are basically composed of various light weight elements and compounds that bonded with the hydrogen atom in binary, ternary, or quaternary structures [1–3]. The binary hydrides are made of light-weight elements and compounds, for example, LiH and MgH_2 often releases the absorbed hydrogen at very high temperatures ($>400^\circ\text{C}$) and are irreversible in nature [4, 5]. The reversibility of hydrogen absorption and desorption can be improved by bringing either the cationic or anionic substitution to form a ternary compound for example, LiBH_4 , Mg_2FeH_6 , or $\text{Zn}(\text{BH}_4)_2$ [6, 7]. Further to decrease the temperature of hydrogen sorption can be facilitated by destabilizing via introducing alkaline metal hydrides, to form a quaternary structure, for example, $\text{LaMg}_2\text{NiH}_7$ [8] or $\text{LiMg}_2\text{RuH}_7$ [9]. There are consistent efforts underway towards the development of a *holy-grail* light weight reversible hydrogen storage materials to meet the 2025 DOE technical targets [10].

Lithium and Magnesium are considered to be lightest and highly reactive elements due to their placement next to hydrogen in the periodic table. The ternary hydride of Lithium, namely, LiBH_4 possesses very high storage density of hydrogen

up to ~20 wt.% and ~ 125 kgH₂/m³ in terms of gravimetric and volumetric measurements [11–14]. However, the significant hydrogen decomposition occurs at temperatures >400°C [15]. The dehydriding and reversible hydriding of LiBH₄ follows the typical metal-hydrogen bonding reactions per the equations below.

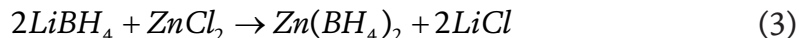


The reversibility enhancements and destabilization of LiBH₄ at lower temperature was demonstrated by admixing of SiO₂ [14], and MgH₂ [16]. Particularly, the addition of half a mole of MgH₂ destabilizes the LiBH₄ structure and enables the formation of intermediate meta-stable MgB₂ alloy phase during the hydrogen release and absorption phases per the equation below [16].



MgH₂ on the other hand, has a comparative hydrogen storage capacity of ~7.6 wt.%, at temperatures >325°C, however, the slow kinetics of reaction makes this metal hydride not usable for potential applications [5]. The role of different 3d transition metal catalysts for example, Ti, V, Mn, Fe, Co, Ni [17–21] and transition metal oxide, namely, Nb₂O₅ [22, 23], has demonstrated greater reversibility of hydrogen from the magnesium lattice with faster kinetics hydrogen enabled applications.

A new ternary complex metal hydride Zn(BH₄)₂, was formulated for the low temperature hydrogen decomposition by reacting either NaBH₄ or LiBH₄ with ZnCl₂ salt in a mechanochemical process at room temperature according to the Equation [24, 25].



Keeping the aforementioned metal hydrides and its salient characteristics, we have successfully synthesized new complex hydrides with combinations of LiBH₄ and MgH₂ for the formation of Zn substituted systems and catalysts assisted complex metal hydrides for reversible hydrogen storage and for vehicular on-board applications.

2. Experimental details

The various chemical compounds with purities (in parentheses) such as, ZnCl₂ (99.999%), TiF₃ (99.999%), nano-Ni (99.9%), nano-Zn (99 + %) are procured from Sigma-Aldrich. The binary and ternary metal hydrides such as LiBH₄ (95%), MgH₂ (98%) are purchased from Alfa Aesar. The high purity nano-Ni (99.999%) was purchased from QuantumSphere Inc. All the chemicals have been stored in a nitrogen filled glove box, used readily without further purification. A mechanochemical milling of the mixtures have been carried out in a Fritsch Pulversitte planetary mono mill P6 using 80 ml stainless steel bowl sealed with a specially designed lid with two scharder valves for inert or reactive gas purging. Various experimental parameters such as ball to powder weight ratio (20:1), milling speed (300 rpm), milling time (20 min. to 2 h) and milling medium (hydrogen purging, 1 atm for every 30 minutes of milling) were optimized. All the sample manufacturing and manipulation for both synthesis and characterization were done in a nitrogen filled glove box (Innovation Technology).

The thermogravimetric and the differential scanning calorimetric analyses were performed using the TA Instrument's SDT-600 with alumina crucibles heated at 5°C/min in flow of nitrogen or argon ambient. The Universal Analysis software V4.0C was deployed to analyze the results obtained from the SDT. The reversible hydrogen absorption and desorption measurements have been carried out using Setaram's PCTPro Sievert's type instrument with pre-calibrated volumes with an accuracy of $\pm 1^\circ\text{C}$. A Lab View software program was used for data monitoring and recording, and the measurement analysis was executed using Hy-Analysis macros in the Igor program.

X-ray diffraction characterization was carried out using a Philips X'pert diffractometer with $\text{CuK}\alpha$ radiation of $\lambda = 5.4060 \text{ \AA}$. The x-ray beam from the cathode ray tube was incident on the sample, via incident slit of 1° , a 10 mm beam mask and soller slit of 0.04 rad. The diffracted x-ray beam was received by the detector via the receiving slit, a 2° anti scatter slit and a monochromator. The collected XRD patterns were analyzed using the PANalytical X'pert Highscore software version 1.0e for phase identification and crystallite size distribution. A polyethylene clear plastic wrap (thin foil) was used to protect the samples from air and moisture by wrapping the sample holder completely with the thin foil which shows diffraction peaks in the 2θ range of $21\text{--}28^\circ$. The chemical environment of the complex metal hydrides, such as B-H stretches and BH_2 deformation bands were explored using a Perkin Elmer's FTIR spectrometer and the samples were specially prepared with KBr in nitrogen filled glove box.

3. Results and discussion

Two different sets of complex metal hydrides have been studied in this work, one is with the mixture, $2\text{LiBH}_4 + \text{ZnCl}_2$ with different catalysts and the other set related to destabilized materials $\text{LiBH}_4 + \frac{1}{2}\text{MgH}_2 + \text{Xmol}\% \text{ZnCl}_2$ with different catalysts. The results of various physicochemical characterizations such TGA, DSC, XRD, FTIR and PCT are discussed for these two sets of complex metal hydrides in the following sub sections.

3.1 Complex metal hydride - $2\text{LiBH}_4 + \text{ZnCl}_2$ without and with different catalysts

The complex metal hydride mixture, $2\text{LiBH}_4 + \text{ZnCl}_2$ was prepared by hand mixing in ceramic mortar and via ball milling for different time duration under inert or reactive ambient. The obtained $\text{Zn}(\text{BH}_4)_2$ per the Eq. (3) was further treated with different catalysts doping. All these as-synthesized materials are then subjected to thermogravimetric and differential scanning calorimetric measurements (TGA-DSC or SDT). **Table 1** represents the onset, and peak temperature of hydrogen decomposition from the complex metal hydride with total weight loss. From the **Table 1**, it is discernible that the pristine mixture $2\text{LiBH}_4 + \text{ZnCl}_2$ milled shows lower hydrogen decomposition temperature by at least 25°C when compared to hand mix counterparts. Additionally, the nano-Ni doping concentration of at least 1–4 mol% on the complex metal hydride mixture shows temperature reduction of at least $15\text{--}20^\circ\text{C}$ for the hydrogen release. Overall, the total gravimetric weight loss due to hydrogen decomposition at the peak temperature, ranges from 12 to 15 wt% of hydrogen was obtained for both undoped and doped complex metal hydride mixtures. The hand mix sample show the weight loss of 9.4 wt.% due to partial formation of $\text{Zn}(\text{BH}_4)_2$. The TGA and DSC profiles as shown in **Figures 1** and **2** supports the **Table 1** results.

Complex Hydride	On-set Temp. °C	Peak Temp. °C	Weight Loss. Wt%
2LiBH ₄ + ZnCl ₂	114.07	125.06	14.80
2LiBH ₄ + ZnCl ₂ + 1 mol% TiF ₃	114.13	129.21	14.92
2LiBH ₄ + ZnCl ₂ + 2 mol% TiF ₃	112.57	128.00	14.18
2LiBH ₄ + ZnCl ₂ + 2 mol% MgH ₂	113.96	128.11	13.70
2LiBH ₄ + ZnCl ₂ Hand mix	138.69	150.50	9.435
2LiBH ₄ + ZnCl ₂ + 1 mol% nanoNi	114.38	116.90	13.54
2LiBH ₄ + ZnCl ₂ + 2 mol% nanoNi	110.38	113.00	14.73
2LiBH ₄ + ZnCl ₂ + 3 mol% nanoNi	106.05	107.30	14.82

Table 1.
TGA-DSC measurements data of pristine and catalyst doped complex metal hydride mixture, 2LiBH₄ + ZnCl₂.

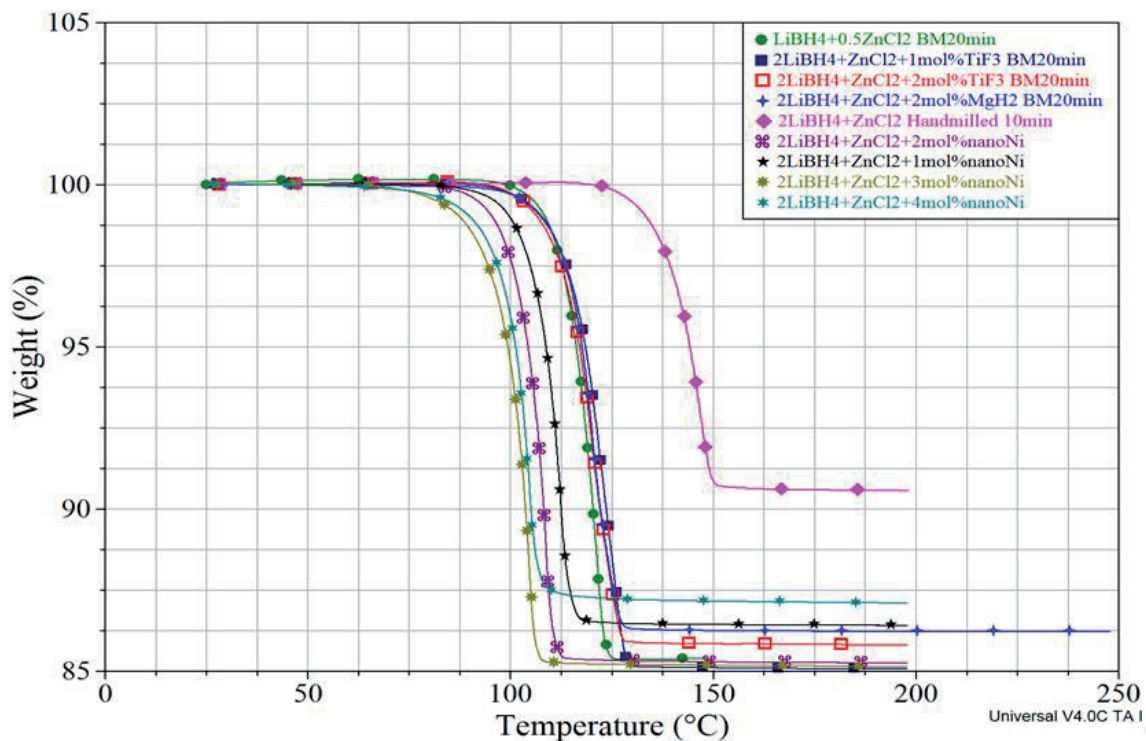


Figure 1.
Thermogravimetric profiles of 2LiBH₄ + ZnCl₂ mixture with different catalysts (up to 4 mol%), such as TiF₃, MgH₂, nano-Ni.

A closer look of the TGA profiles (**Figure 1**), one can find a detailed observation as follows. Comparison between the metal hydride mixtures, LiBH₄ + ½ ZnCl₂ ball milled for 20 minutes shows greater hydrogen release at lower temperatures than the sample, 2LiBH₄ + ZnCl₂ hand mixed for 10 minutes, which emphasize the need of mechanical milling to complete the reaction stated in Eq. (3). Regarding the different concentrations of TiF₃, 2 mol% reveals at least 0.5% more of hydrogen release and at temperatures at least 1°C lesser than the concentration 1 mol% TiF₃. For the 2 mol% MgH₂ doping, which showed similar performance like TiF₃ dopant in terms of both thermal decomposition temperature and weight loss characteristics and are inferior to the pristine LiBH₄ + ½ ZnCl₂ mixture milled for 20 minutes. Nano-nickel on the other hand, doping with different concentrations, 1–4 mol%, demonstrated

superior thermal decomposition behavior with 3 mol% as an optimum concentration as shown in **Figure 1**.

The DSC profiles as exhibited in **Figure 2**; the endothermic peaks are due to thermal hydrogen decomposition where the weight loss was observed in **Figure 1**. As it is mentioned that the partial reaction of the hand mixed compounds as noted earlier is supported well with the DSC studies in which there were two endo- peaks obtained, one may be due to the LiBH_4 phase and other may be due to the partial $\text{Zn}(\text{BH}_4)_2$ phase. However, the ball milled samples show only one endo sharp peak, the area under this curve enhanced at lower temperatures, by nano-Ni catalyst doping as shown in **Figure 2**.

The x-ray diffraction patterns of all the samples listed in **Table 1** are carried out with the similar experimental conditions and background parameters and are depicted in **Figure 3**. It is very well confirmed from the XRD profiles that the hand mix metal hydride samples show the existence of unreacted LiBH_4 and ZnCl_2 . Whereas, the ball milled counterparts reveals the appearance of by-product, LiCl , thus the consumption or reaction of 2LiBH_4 and ZnCl_2 to produce a new $\text{Zn}(\text{BH}_4)_2$ compound, with unknown peak appeared at around 20.5° . For the catalysts, doped $2\text{LiBH}_4 + \text{ZnCl}_2$, the peaks correspond to TiF_3 , or nano-Ni are not visible due to the low concentration (<4 mol%), and the XRD patterns were very similar to the pristine complex metal hydride ball milled for 20 minutes. The presence of LiCl phase affects the total hydrogen storage capacity reported in **Table 1**, because of the dead weight contribution from the LiCl . Overall, the XRD profiles of the complex metal hydrides supports the reaction (3) and the thermal characteristics as discussed above.

3.2 Complex Metal Hydride - $\text{LiBH}_4 + \frac{1}{2}\text{MgH}_2 + \text{Xmol}\% \text{ZnCl}_2$

Based on the by-product LiCl appearance in the reaction discussed in Section 3.1 and to enhance the hydrogen storage capacity, the concentration of ZnCl_2 was

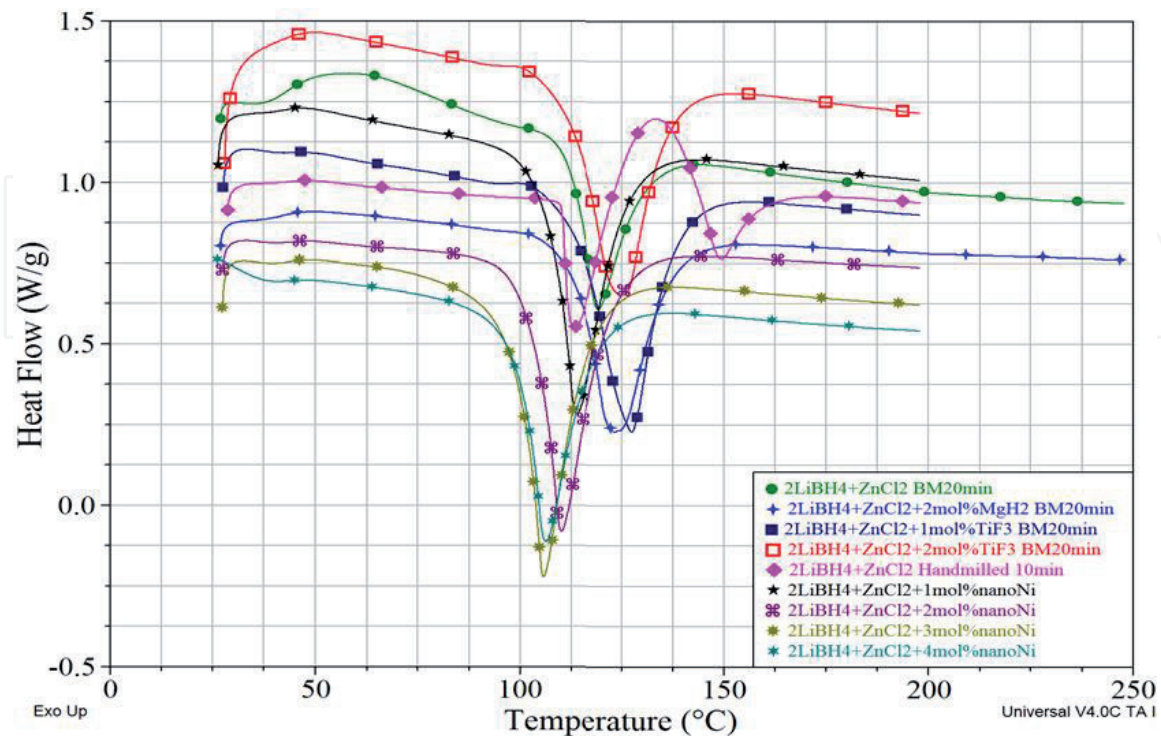


Figure 2. Differential Scanning Calorimetric profiles of $2\text{LiBH}_4 + \text{ZnCl}_2$ mixture with different catalysts (up to 3 mol%), such as TiF_3 , MgH_2 , nano-Ni.

reduced in steps of few mol% on the $\text{LiBH}_4 + \frac{1}{2}\text{MgH}_2$ complex metal hydride system. LiBH_4 and MgH_2 were ball milled (2 hours) together with 1:0.5 ratio and ZnCl_2 have been admixed with different mol% concentrations to form complex composite hydride, $\text{LiBH}_4 + \frac{1}{2}\text{MgH}_2 + X\text{mol}\% \text{ZnCl}_2$ ($X = 0, 2, 4, 6, 8$ and 10). **Figure 4** represents the XRD patterns of the complex metal hydride with different value of X . When $X = 0$, with no ZnCl_2 , the structure is more or less the mixture of LiBH_4 and MgH_2 . However, if the value of X increases to 2 mol%, the appearance Zn peak and the reduction of LiBH_4 relative intensity are observed. For $X = 4$, an unknown peak appears around 20.5° because of the reaction of

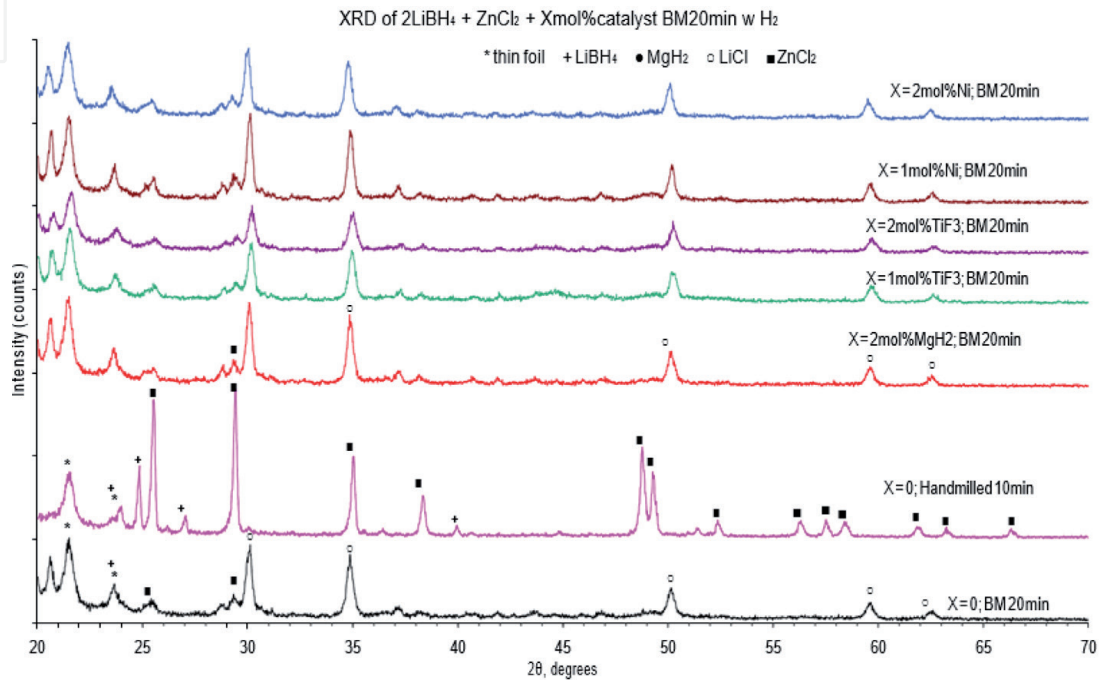


Figure 3. X-ray diffraction patterns of $2\text{LiBH}_4 + \text{ZnCl}_2$ mixture without and with different catalysts (1–4 mol% concentrations).

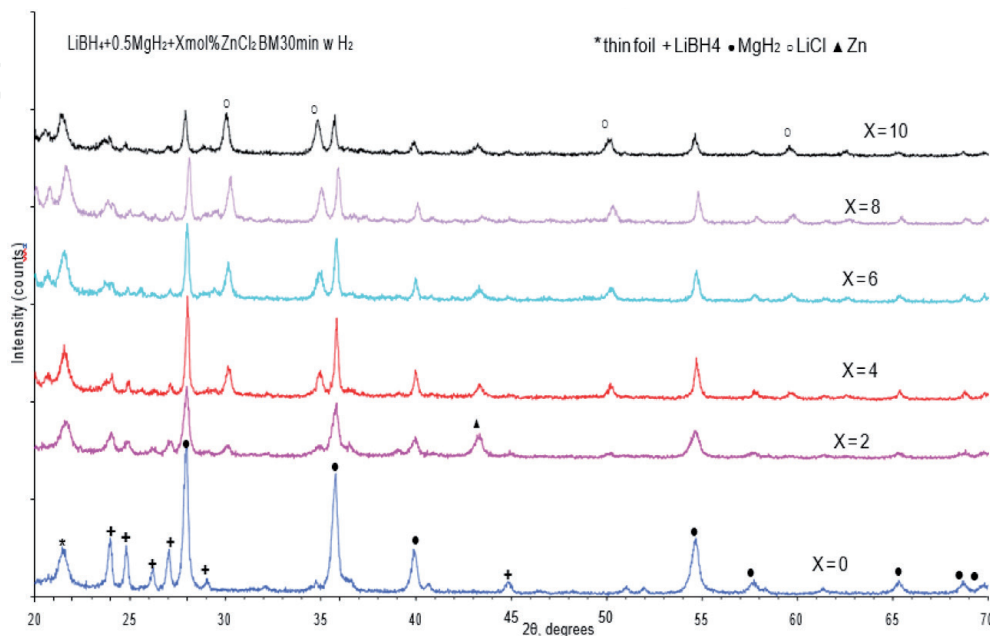


Figure 4. XRD profiles of $\text{LiBH}_4 + \frac{1}{2}\text{MgH}_2 + X\text{mol}\% \text{ZnCl}_2$ ball milled for 30 min in reactive (H_2) atmosphere.

LiBH_4 and available Zn to form $\text{Zn}(\text{BH}_4)_2$ as per the Eq. (3) and hence the by-product formation of LiCl was inevitable. For the X value of 10 mol%, the LiBH_4 phase and the pure Zn phase drastically reduced, however there was no changes in the MgH_2 structural phase. Therefore, the XRD profiles confirm the Eq. (3) with concentration optimization of ZnCl_2 which could further control the by-product LiCl formation. The Fourier Transform Infrared (FTIR) Spectroscopic profiles of $\text{LiBH}_4 + \frac{1}{2}\text{MgH}_2 + X\text{mol}\% \text{ZnCl}_2$ ($X = 0, 2, 4, 6, 8$ and 10) shows the presence of B-H stretch, at wavenumbers, 2276 cm^{-1} and 2213 cm^{-1} and another peak

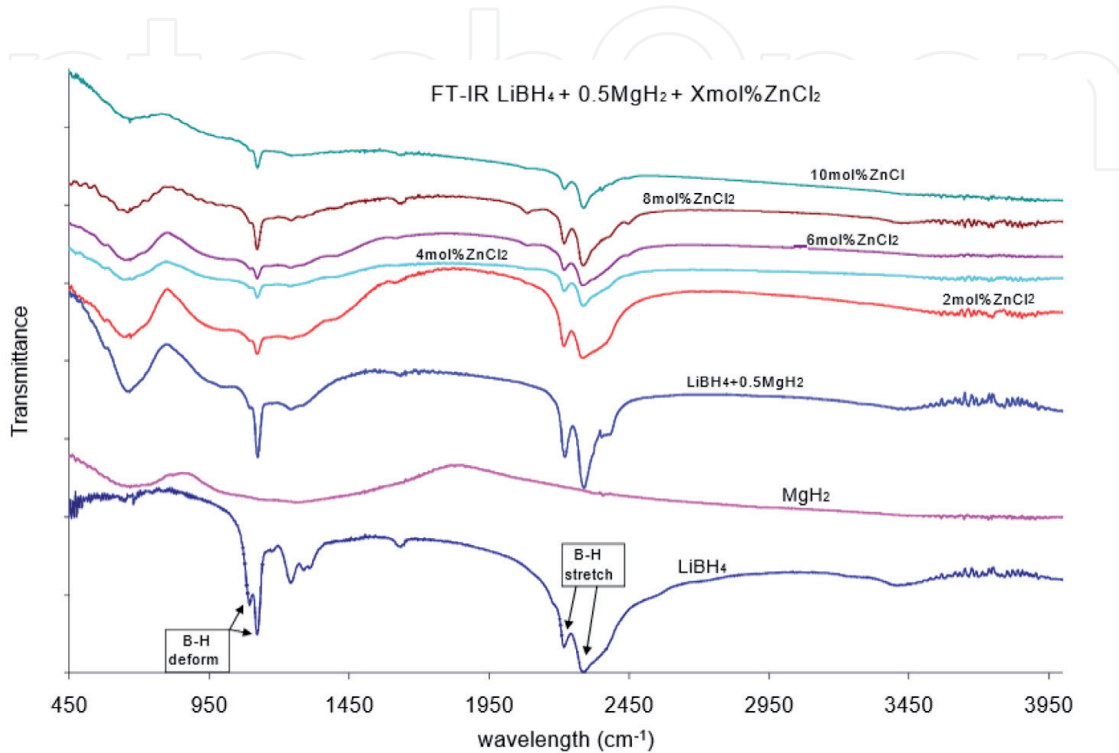


Figure 5. FTIR of $\text{LiBH}_4 + \frac{1}{2}\text{MgH}_2 + X\text{mol}\% \text{ZnCl}_2$ ($X = 0, 2, 4, 6, 8$ and 10) ball milled for 30 min in reactive (H_2) atmosphere.

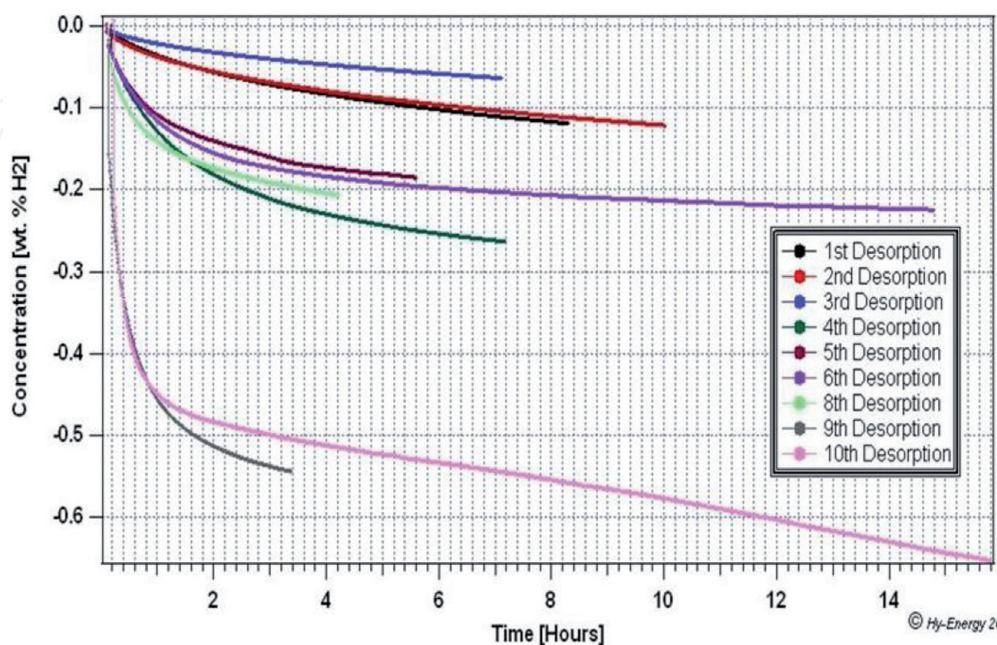


Figure 6. Desorption Data Collected on a PCT for $\text{LiBH}_4 + \frac{1}{2}\text{MgH}_2 + 2 \text{ mol}\% \text{ZnCl}_2$ Ball Milled 2 Hours Under H_2 Ambient.

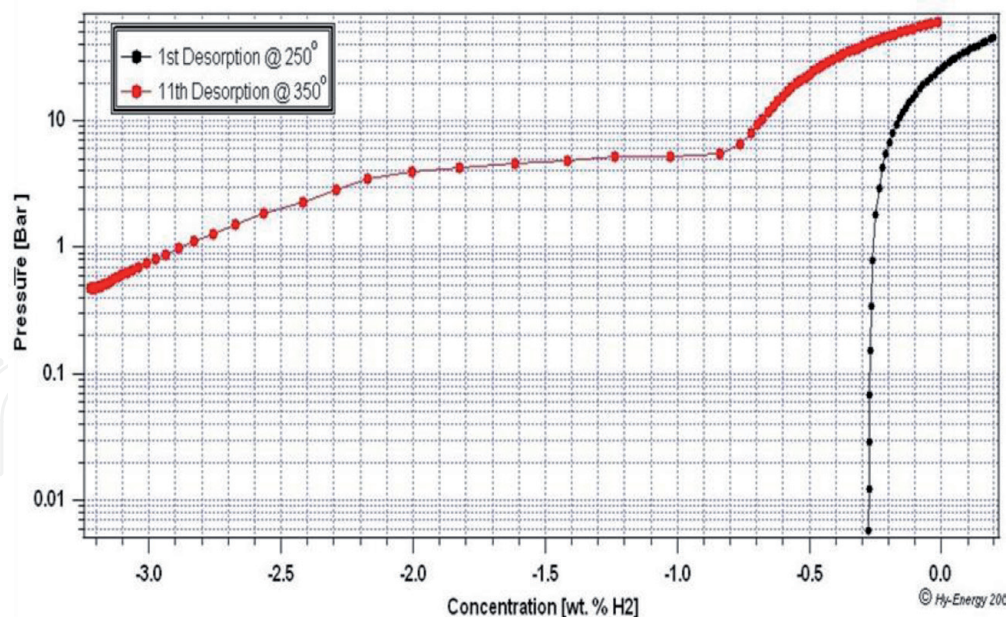


Figure 7. PCT Desorption at 250°C and 350°C for the mixture, $\text{LiBH}_4 + \frac{1}{2}\text{MgH}_2 + 2 \text{ mol\% ZnCl}_2$ Ball Milled 2 Hours Under H_2 Ambient.

correspond to BH_2 deformation band was observed at 1118 cm^{-1} and 1091 cm^{-1} due to LiBH_4 (see **Figure 5**). These stretches were decreased in transmittance values when X increases from 2 to 10 mol%. No additional impurity peaks were observed.

The hydrogen absorption and desorption characteristics of $\text{LiBH}_4 + \frac{1}{2}\text{MgH}_2 + 2 \text{ mol\% ZnCl}_2$ was demonstrated using the PCT Sievert's type apparatus. The hydrogen desorption experiments were performed at various temperatures, for example from 1 to 3 cycles at 250°C, 4–6 cycles at 300°C and 8–10 cycles at 350°C. As the temperatures increased from 250–350°C, the hydrogen storage capacity increases five-fold as shown in **Figure 6**. At the end of each desorption run, the sample was hydrogenated at high pressure, up to 40 atmosphere and at temperature of 200°C for several hours. The PCT isotherm of 11th desorption run at 350°C demonstrates the plateau pressure of hydrogen desorption, at around 4–5 bars and the storage capacity of ~3.0 wt.% (see **Figure 7**). Based on the aforementioned characteristics, these complex metal hydrides bearing light weight elements or compounds, for example LiBH_4 and MgH_2 with catalysts dopants may be considered as potential applications for clean energy or fuel (hydrogen) storage.

4. Conclusion

Two sets of complex metal hydrides comprising light weight elements and compounds have been prepared via solid state mechanochemical process. The transition metal chloride, for example, ZnCl_2 addition to LiBH_4 in the ratio of 1;2, ends up forming a new complex hydride, $\text{Zn}(\text{BH}_4)_2$ with thermal decomposition of hydrogen release at lower temperatures, $<130^\circ\text{C}$ and high hydrogen capacity $>10 \text{ wt.\%}$. The 1:0.5 ratio of $\text{LiBH}_4:\text{MgH}_2$ (and 2 mol% ZnCl_2) in this complex structure thus destabilizes and maintain the plateau pressure, 4–5 atmospheres for the hydrogen desorption with total reversible hydrogen storage capacity ~3.0 wt.% at around 350°C. The structural and chemical characteristics of $\text{LiBH}_4 + \frac{1}{2}\text{MgH}_2 + 2 \text{ mol\% ZnCl}_2$ and other concentration variations, including catalytic doping via nano-Ni shows reversible hydrogen storage behavior.

Acknowledgements

The authors are grateful to the respective institutions, Florida Polytechnic University and University of South Florida for students' support and research infrastructures. Funding sources, US Department of Energy, Florida Energy Systems Consortium and Hinkley Center for Solid and Hazardous Waste Management are gratefully acknowledged.

Conflict of interest

The authors declare no conflict of interest.

Author details

Sesha Srinivasan^{1*}, Luis Rivera², Diego Escobar³ and Elias Stefanakos⁴

¹ Department of Natural Sciences, Florida Polytechnic University, Lakeland, Florida, USA


² Environmental/Mechanical Engineering, Fleet Standards Branch, Military Sealift Command, Norfolk, USA

³ Department of Field Services, Tigo Colombia, Medellin, Colombia

⁴ Clean Energy Research Center, College of Engineering, University of South Florida, Tampa, Florida, USA

*Address all correspondence to: ssrinivasan@floridapoly.edu

IntechOpen

© 2021 The Author(s). Licensee IntechOpen. This chapter is distributed under the terms of the Creative Commons Attribution License (<http://creativecommons.org/licenses/by/3.0>), which permits unrestricted use, distribution, and reproduction in any medium, provided the original work is properly cited. 

References

- [1] Guzik MN, Mohtadi R, Sartori S. Lightweight complex metal hydrides for Li-, Na- and Mg- based batteries. *J. Materials Research*. 2019;34:6:877-904. DOI: 10.1557/jmr.2019.82
- [2] Schuth F, Bogdanovic B, Felderhoff M. Light metal hydrides and complex hydrides for hydrogen storage. *Chem. Comm*. 2004:2249-2258. DOI: 10.1039/B406522K
- [3] Moller KT, Sheppard D, Ravisbaek DB, Buckley CE, Akiba E, Hi H-W, Jensen TR. Complex metal hydrides for hydrogen, thermal and electrochemical energy storage. *Energies*. 2017;10:1645:1-30. DOI: 10.3390/en10101645
- [4] Bourgeois N, Crivello J-C, Cenedese P, Joubert J-M. Systematic first-principles study of binary metal hydrides. *ACS Comb. Sci*. 2017;19:8"513-523. DOI: 10.1021/acscombsci.7b00050
- [5] Grochala W, Edwards P. Thermal decomposition of non-interstitial hydrides for the storage and production of hydrogen. *Chem. Rev*. 2004;104:1283-1315. DOI: 10.1021/cr030691s
- [6] Yamaguchi M, Akiba E. Ternary hydrides. In: *Materials Science and Technology*. Wiley-VCH Verlag GmbH & Co KGaA; 2006. DOI: 10.1002/9783527603978.mst0043
- [7] Bronger W. Complex transition metal hydrides. *Angewandte Chemie International Edition*. 1991;L30:7:759-768. DOI: 10.1002/anie.199107591
- [8] Renaudin G, Guenee L, Yvon K. $\text{LaMg}_2\text{NiH}_7$, a novel quaternary metal hydride containing tetrahedral $[\text{NiH}_4]^{4-}$ complexes and hydride anions. *J. Alloys and Compounds*. 2003;350:145-150. DOI: 10.1016/S0925-8388(02)00963-5
- [9] Huang B, Yvon K, Fischer P. $\text{LiMg}_2\text{RuH}_7$, a new quaternary metal hydride containing octahedral $[\text{Ru}(\text{H})\text{H}_6]^{4-}$ complex anions. *J. Alloys and Compounds*. 1994;210:1-2:243-246. DOI: 10.1016/0925-8388(94)90144-9
- [10] DOE Technical Targets for Onboard Hydrogen Storage for Light-Duty Vehicles [Internet]. 2020. Available from: <https://www.energy.gov/eere/fuelcells/doe-technical-targets-onboard-hydrogen-storage-light-duty-vehicles>
- [11] Zuttel A, Rentsch S, Fisher P, Wenger P, Sudan P, Mauron Ph, Emmenegger Ch. Hydrogen storage properties of LiBH_4 . *J. Alloys and Compounds*. 2003;356-357:515-520. DOI: 10.1016/S0925-8388(02)01253-7
- [12] Schlesinger HI, Herbert CB. Metallo borohydrides. III. Lithium borohydride. *J. Am. Chem. Soc*. 1940;62:12:3429-3435. DOI: 10.1021/ja01869a039
- [13] Kong VCY, Foulkes FR, Kirk DW, Hinatsu JT. Development of hydrogen storage for fuel cell generators, i. hydrogen generation using hydrolysis hydrides. *Int. J. Hydrogen Energy*. 1999;24:7:665-675. DOI: 10.1016/S0360-3199(98)00113-X
- [14] Kojima Y, Kawai Y, Kimbara M, Nakanishi H, Matsumoto S. Hydrogen generation by hydrolysis reaction of lithium borohydride. *Int. J. Hydrogen Energy*. 2004;29:12:1213-1217. DOI: 10.1016/j.ijhydene.2003.12.009
- [15] Orimo S, Nakamori Y, Gitahara G, Miwa K, Ohba N, Towata S, Zuttel A. Dehydriding and rehydriding reactions of LiBH_4 . *J. Alloys and Compounds*. 2005;404-406:427-430. DOI: 10.1016/j.jalcom.2004.10.091
- [16] Vajo JJ, Skeith SL, Mertens F. Reversible storage of hydrogen in destabilized LiBH_4 . *J. Phys. Chem. B*. 2005;109:9:3719-3722. DOI: 10.1021/jp040769o

- [17] Huot J, Liang G, Boily S, Van Neste A, Schulz R. Structural study and hydrogen sorption kinetics of ball-milled magnesium hydride. *J. Alloys and Compounds*. 1999;293-295:495-500. DOI: 10.1016/S0925-8388(99)00474-0
- [18] Liang G, Huot J, Boily S, Van Neste A, Schulz R. Hydrogen storage properties of the mechanically milled MgH₂-V nanocomposite. *J. Alloys and Compounds*. 1999;291:1-2:295-299. DOI: 10.1016/S0925-8388(99)00268-6
- [19] Liang G, Huot J, Boily S, Schulz R. Hydrogen desorption kinetics of a mechanically milled MgH₂+5at.%V nanocomposite. *J. Alloys and Compounds*. 2000;305:1-2:239-245. DOI: 10.1016/S0925-8388(00)00708-8
- [20] Dehouche Z, Djaozandry R, Huot J, Boily S, Goyette J, Bost TK, Schulz R. Influence of cycling on the thermodynamic and structure properties of nanocrystalline magnesium-based hydride. *J. Alloys and Compounds*. 2000;305:1-2:264-271. DOI: 10.1016/S0925-8388(00)00718-0
- [21] Huot J, Pelletier JF, Liang G, Scutton M, Schulz R. Structure of nanocomposite metal hydrides. *J. Alloys and Compounds*. 2002;330-332:727-731. DOI: 10.1016/S0925-8388(01)01662-0
- [22] Barkhordarian G, Klassen T, Bormann R. Fast hydrogen sorption kinetics of nanocrystalline Mg using Nb₂O₅ as catalyst. *Scripta Materialia*. 2003;49:3:213-217. DOI: 10.1016/S1359-6462(03)00259-8
- [23] Barkhordarian G, Klassen T, Bormann R. Effect of Nb₂O₅ content on hydrogen reaction kinetics of Mg. *J. Alloys and Compounds*. 2004;304:1-2:242-246. DOI: 10.1016/S0925-8388(03)00530-9
- [24] Jeon E, Cho YW. Mechanochemical synthesis and thermal decomposition of zinc borohydride. *J. Alloys and Compounds*. 2006;422:1-2:273-275. DOI: 10.1016/j.jalcom.2005.11.045
- [25] Srinivasan S, Escobar D, Jurczyk M, Goswami Y, Stefanakos E. Nanocatalyst doping of Zn(BH₄)₂ for on-board hydrogen storage. *J. Alloys and Compounds*, 2008;462:1-2:294-302. DOI: 10.1016/j.jallcom.2007.08.028